

Borehole Seismic Monitoring of Injected CO₂ at the Frio Site

Thomas M. Daley, Larry R. Myer, G.M. Hoversten, John E. Peterson,
Valeri A. Korneev

Lawrence Berkeley National Laboratory, Berkeley Ca., USA

Abstract

As part of a small scale sequestration test (about 1500 tons of CO₂) in a saline aquifer, time-lapse borehole seismic surveys were conducted to aid in characterization of subsurface CO₂ distribution and material property changes induced by the injected CO₂. A VSP survey demonstrated a large increase (about 75%) in seismic reflectivity due to CO₂ injection and allowed estimation of the spatial extent of CO₂ induced changes. A crosswell survey imaged a large seismic velocity decrease (up to 500 m/s) within the injection interval and provided a high resolution image of this velocity change which maps the subsurface distribution of CO₂ between two wells. Numerical modeling of the seismic response uses the crosswell measurements to show that this small CO₂ volume causes a large response in the seismic reflectivity. This result demonstrates that seismic detection of small CO₂ volumes in saline aquifers is feasible and realistic.

Keywords: CO₂, sequestration, borehole seismic, monitoring, saline aquifer

Introduction

As part of a Department of Energy (DOE) funded project on geologic sequestration of CO₂, borehole seismic surveys were acquired before and after injection of about 1500 tons of CO₂ into a saline aquifer.

The seismic surveys consisted of Crosswell and vertical seismic profile (VSP) experiments, which were part of an integrated suite of scientific studies with many contributing institutions including the Texas Bureau of Economic Geology who performed the site selection process.

The injection site was selected in 2003 after characterization of 21 representative saline formations in the onshore United States. The selected aquifer is part of the on-shore Gulf of Mexico Frio formation sandstone, near Houston, Tx. The experimental site is in a historical oil field, where site access, use of an idle well as an observation well, wireline well logs, 3-D seismic, and production data were donated by the operator, Texas American Resources.

Among the goals of the CO₂ injection were the following: 1) Demonstrate that CO₂ can be injected into a brine formation without adverse health, safety, or environmental effects; 2) Determine the subsurface distribution of injected CO₂; 3) Demonstrate validity of conceptual models; 4) Develop experience necessary for the success of large-scale injection.

The borehole seismic surveys were each designed to augment these goals with the following:

Crosswell: 1) Spatial mapping of CO₂ between wells; 2) Measure change in mechanical properties of the reservoir; 3) Combine with other measurements to estimate CO₂ saturation between wells.

VSP: 1) Imaging of nearby structure (faults, etc); 2) Spatial mapping of CO₂ beyond the well pair.

The VSP and crosswell were acquired together, with pre-injection surveys in July 2004 and post-injection suveys in November 2004, about 1.5 months after the injection ended.

Geologic Background and Characterization

Sandstones of the Oligocene Frio Formation are a target for large-volume storage because they are part of a thick, regionally extensive sandstone trend that underlies a concentration of industrial

sources and power plants along the Gulf Coast of the United States. However, the specific site selected was optimized for a small demonstration, and the injection well is not suitable for, nor was it ever intended to be, a full-scale injection project. Detailed characterization was conducted using traditional reservoir assessment tools [1]. This effort included use of seismic and log analysis to define facies, structure, and diagenetic evolution and estimation of petrophysical and geochemical properties using core to build a quantitative reservoir model. From this characterization, a numerical model was created using LBNL's TOUGH2 code. Geologically constrained numerical models of injection and monitoring scenarios were prepared and used to optimize the experimental design, well locations and completion, and monitoring tool selection. The Frio "C" sandstone, a 23-m-thick brine-bearing interval above oil production was selected as the injection target.

The upper Frio in this area is composed of northwest-southeast-elongated fluvial sandstone separated by mudstones and shales that can be correlated over the field but not regionally. The upper Frio "C," "B," and "A" (in lower to upper stratigraphic order) sandstones are part of a trend of fluvial sandstones that were increasingly reworked beneath the regionally extensive 60-m-thick (200-ft) shales and mudstones of the overlying Anahuac Formation. The selected injection zone, the upper half of the Frio "C" sandstone, is an 22.8-m (75-ft) upward-fining, fine-grained, poorly indurated, well-sorted sandstone at a depth of about 1500 m.

The massive upper part of the upper "C" sandstone has porosities of 30 to 35% and permeabilities of 2,000 to 2,500 md. Finer grained and more layered sandstone and clayey sandstone having porosities of 24 to 28% and permeabilities of 70 to 120 md make up the mid-"C" and the top "C" transition to the top "C" seal. The top "C" seal is composed of shale, sands, and siltstones that form a minor seal beneath the regional Anahuac Shale but probably a major barrier to vertical flow out of the "C" sandstone.

Structural analysis of the injection interval using logs and a 3-D seismic volume shows that the upper Frio Formation at the test site is within a fault-bounded compartment that is part of a system of radial faults above the salt dome. Dips within the injection compartment are steep. Hand-picked interpretation of the FMI log by Schlumberger measured dips of 18 degrees to the south at the injection well; interwell correlation measured an average dip of 16 degrees south. Neither FMI nor seismic surveys identified fractures or faults in the interwell area, although the steep dip is compatible with deformation band structures interpreted in core C-T scans.

Seismic Data Acquisition

The VSP and crosswell use different acquisition geometries. Figure 1a shows the VSP geometry which has a surface source and borehole sensors recording direct and reflected energy. Figure 1b shows the crosswell geometry which has borehole sources and borehole sensors. The crosswell survey has higher resolution because of the subsurface source and (typically) shorter distances. However the crosswell is limited to the interwell volume while the VSP can potentially image on any azimuth and with offsets of about one-half of the well depth.

Both the VSP and crosswell surveys used an 80-level 3-component geophone string, which was supplied by Paulsson Geophysical and deployed on special tubing. For the crosswell survey, the source was an orbital vibrator, supplied by LBNL. The source and receiver spacing was 1.5 m, with the sources spanning 75 m and the sensors spanning 300 m. Five source 'fans' were acquired to give 1.5 m sensor spacing from the 7.5 m fixed sensor spacing. The crosswell survey was conducted using the injection well (for sensors) and the nearby monitoring well (for source) which is about 30 m offset. Crosswell source locations were centered on the injection interval. The crosswell sensors were also centered on the injection interval, which is about 6-7 m thick.

The orbital vibrator source is an eccentric mass rotated by an electric motor. The source is fluid coupled to the surrounding formation. The rate of rotation is linearly varied up to 350 Hz and back to stop. Useable energy is acquired above about 70 Hz, giving a 70 to 350 Hz bandwidth. At each source location a clockwise and counter clockwise sweep is recorded. Decomposition of these

two sweeps provides two equivalent sources with orthogonal horizontal oscillations [2]. Component rotation using P-wave particle motion rotates these two sources into in-line and cross-line equivalents, with in-line being horizontal and in the plane of the two boreholes [3]. This rotation results in a 6-component receiver gather with in-line and cross-line sources for the vertical and two horizontal receiver components. The in-line source generates predominantly P-wave energy while the cross-line source generates predominantly S-wave energy. Consistent generation of both P- and S-waves is a notable feature of the orbital vibrator source.

The VSP used the same 80 level, 3-component geophone string and explosive sources. Eight source shot points were acquired (Figure 2). The sensors were interleaved to give spacings of 1.5 to 7.5 m. Comparison of variable sensor spacing shows advantage for increasing spatial sampling. The shotpoints were offset 100 to 1500 m from the sensor well. The location of the shotpoints (Figure 2) was designed to monitor the estimated CO₂ plume location (VSP sites 1-4) and to provide structural information at the injection site (sites 5-9).

Data Processing and Analysis

The processing of the VSP has focused on time lapse change in reflection amplitude of the reservoir horizon. Initial processing includes applying time shifts to correct for shot variations, picking of arrival times at each depth, separation of down-going and up-going (reflected) wavefields, converting reflections to two-way travel time and enhancing the reflected energy signal. Following these processing steps, an amplitude equalization was applied using a reflection above the reservoir, thereby removing the time-lapse changes due to near surface and shallow sub-surface variation (such as soil moisture saturation). At this point the time-lapse change reservoir reflection can be analyzed. The result from one source location is shown in Figure 3 where we see a clear increase in the reflection strength from the Frio formation reflection. Similar results have been found from the other source points. For the VSP geometry, the reflection recorded at each sensor in the well originates at a different reflection point, so we are able to estimate the variation in reflection strength with offset along the azimuth between source and borehole.

The VSP reflection change along three azimuths has been spatially mapped using ray tracing to give an estimate of the reflection point location. Figure 4a shows this estimate for a single azimuth with a comparison to the CO₂ saturation estimated at the same offset and azimuth using a numerical flow model [1]. We see a good qualitative agreement of the plume extent, about 80 m radially. Figure 4 b shows this same comparison on three azimuths, North, Northwest and Northeast. We see that there is good agreement to the North, fair to the Northeast and worse to the Northwest. Since the numerical model is laterally homogeneous, the disagreement indicates lateral heterogeneity imaged by the VSP which is not captured in the model.

The crosswell data shows good quality P- and S-wave direct arrivals, allowing velocity tomography. The travel times were picked using the in-line source for P-wave and the cross-line source for S-wave. During the post-injection travel time picking, a large change in waveforms was observed in the injection zone. Because this change was interpreted as 'guided waves' generated by a newly formed low-velocity zone, travel times within this zone were not used for inversion of time-lapse changes. Guided waves do not follow the ray-theory used in standard tomographic inversion. Using the remaining picked travel times, tomographic imaging of velocity was performed. The tomography had the following details: limited ray angles (no vertical offsets greater than 100 m), correction for the deviation of the boreholes from vertical, a straight ray projection, and a static correction to allow for borehole effects. Importantly, the data were inverted for the change in velocity, rather than inverting for each velocity field and then differencing. We have found that this improves the resolution of temporal changes. The inversion used a 2 m x 2m pixel size, with plotting interpolated to 0.5 m. Figure 5 shows the tomographic image of P-wave velocity change, along with the well logs indicating CO₂ saturation near the boreholes. The well logs are Schlumberger's reservoir saturation tool (RST) [4]. The CO₂ plume is clearly imaged by the velocity change, and the spatial agreement between the well logs and the tomograms provides

mutual corroboration to each of these two independent measures of CO₂.

Interpretation

The injection of CO₂ causes a fluid substitution within the pore space. For fluid substitution with no change in matrix properties, a change in P-wave velocity with minimal change in S-wave velocity is expected (a small change in S-wave velocity is due to the change in fluid density). Time-lapse tomographic imaging did map changes in P-wave velocity (over 500 m/s) due to the CO₂ plume (Figure 5). The S-wave tomogram shows minimal change, as expected, except at the injection well near the perforations. The variation in P-wave velocity change is interpreted as resulting from changes in CO₂ saturation. Quantitative estimation of CO₂ saturation from the change in seismic velocity is an ultimate goal, and such estimates can be obtained using a rock physics model. For our site, core studies typically performed to build a rock physics model have not yet been performed and the unconsolidated sand limited core recovery. Similarly, well log measurement of seismic velocity change, which could be closely tied to well log estimates of saturation (the RST log), failed to give useable results for post-injection. Therefore, quantitative saturation estimates from seismic measurements are limited and have large variations.

The large VSP reflection response was somewhat unexpected because of the small spatial size of the CO₂ plume (about 5-7 m thick at 1500 m depth). To verify the result we developed a numerical model of wave propagation, inserted the velocity change measured by the crosswell survey, and analyzed the time-lapse VSP response. The modeling used a 2-D elastic, finite-difference wave propagation code on a 201 by 652 grid with 5 m grid points (1 km by 3.3 km) and a 30 Hz center frequency. The initial 2-D velocity structure was built using horizons mapped from previous surface seismic, velocities measured by the pre-injection VSP, and velocity and density measured by pre-injection well logs. VSP data was generated using this pre-injection model. Then a 400 m/s velocity decrease was applied to a 4 m thick zone across the entire model. A second model applied the heterogeneous crosswell measured change in the 30 m wide zone between wells. For both models, a 'post-injection' VSP data set was calculated. The 'time-lapse' VSP response was calculated using the same processing as the field data, with the exception of amplitude calibration to a shallower reflection, which is unnecessary for numerical data with no shallow changes. The modeled time-lapse VSP response is shown in Figure 6 and bounds the field measurement. This result demonstrates that the velocity changes, as imaged by crosswell tomography, are able to generate the large reflection amplitude change observed in the VSP, when they are extended beyond the interwell region.

Conclusions

Borehole seismic acquisition at the Frio site provided in-situ estimates of the spatial distribution of injected CO₂, with high resolution imaging between injection and monitoring wells (crosswell), and lower resolution at larger distances, on different azimuths (VSP). Numerical modeling of the seismic response uses the crosswell measurements to show that this small CO₂ volume causes a large response in the seismic reflectivity measured with VSP. It is reasonable to infer that the large reflection response seen in the VSP would allow surface seismic monitoring, allowing monitoring away from boreholes. This result demonstrates that seismic detection of small CO₂ volumes in saline aquifers is feasible and realistic.

Acknowledgement:

This work was supported by the GEOSEQ project for the Assistant Secretary for Fossil Energy, Office of Coal and Power Systems through the National Energy Technology Laboratory, of the US Department of Energy, under Contract No. DE-AC02-05CH11231.

Reference list:

- [1] Hovorka, S.D., Benson, S.M., Doughty, C., Freifeld, B.M., Sakurai, S., Daley, T.M., et al., 2006, Measuring permanence of CO₂ storage in saline formations: the Frio experiment,

[2] Daley, T.M. and Cox, D., 2001, Orbital vibrator seismic source for simultaneous P- and S-wave crosswell acquisition, *Geophysics*, 66, 1471-1480.

[3] Gritto, R., T.M. Daley, and L.R. Myer, 2004, Joint cross well and single well seismic studies at Lost Hills, California. *Geophysical Prospecting*, 52, p323-339

[4] Muller, N., Ramakrishnan, T.S., Sakurai, S., Boyd, A., 2005, Time-lapse CO₂ monitoring with pulsed neutron logging, *Fourth Annual Conference on Carbon Capture and Sequestration*, May 2-5, 2005, Alexandria, Virginia.

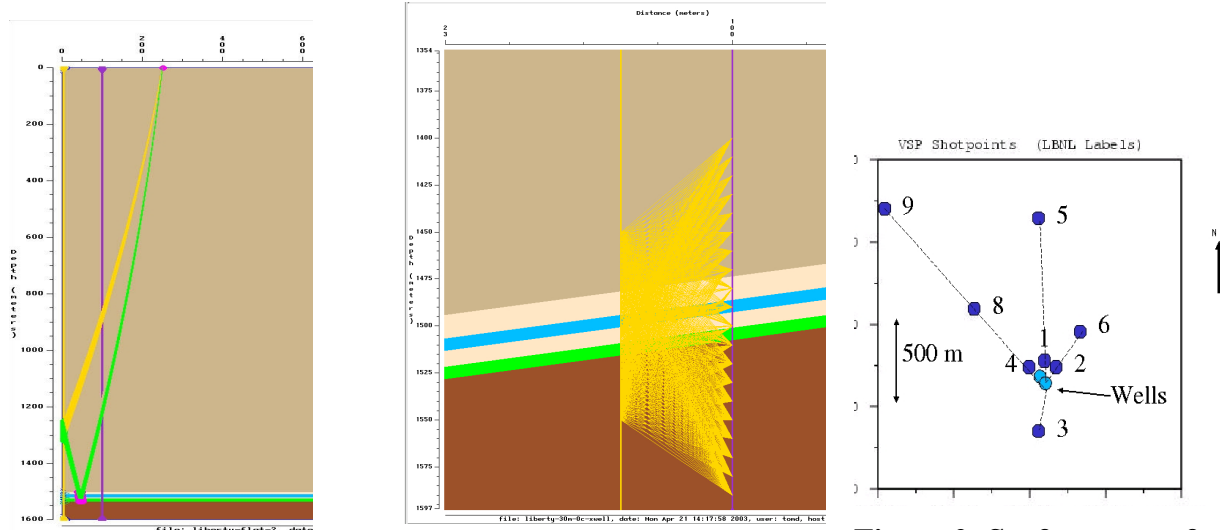


Figure 1a (left) Example of VSP geometry showing raypaths (yellow and green) from a surface source to borehole sensors. The green rays are reflected from interfaces.

Figure 1B(right) Example of crosswell geometry showing raypaths (yellow) for sources (right side) and sensors (left side) in two separate boreholes. Area covered by raypaths can be tomographically imaged.

Figure 2: Surface map of VSP source point locations (dark blue) and wells (light blue).

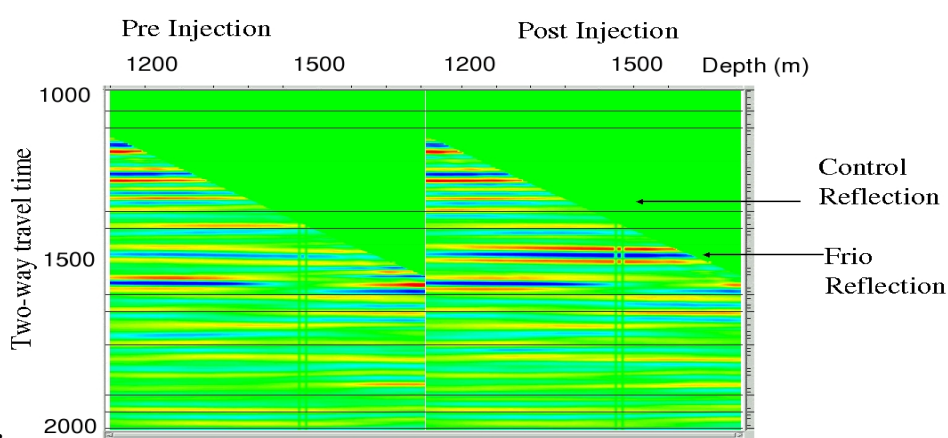


Figure 3: VSP reflections for pre-injection (left) and post-inject (right) after amplitude normalization using the control reflection. The change in amplitude in the Frio reflection is due to CO₂ injection.

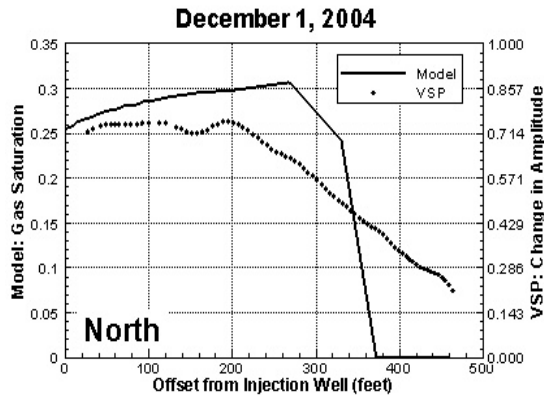


Figure 4a: Numerically modeled CO_2 saturation as a function of offset from the injection well, along with recorded change in VSP reflection amplitude at the same offsets.

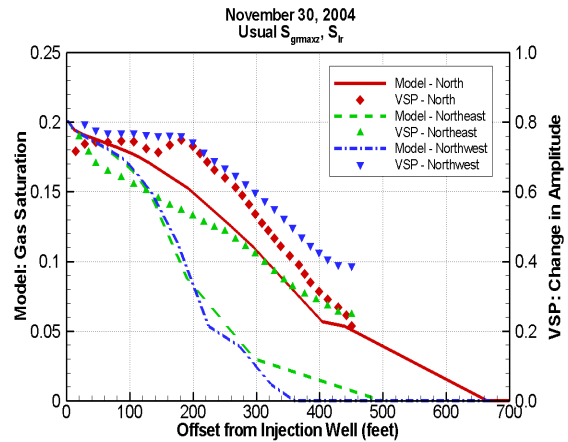


Figure 4b: Modeled CO_2 saturation and recorded VSP amplitude change, as a function of offset, for 3 azimuths, North (red), Northeast (green) and Northwest (blue).

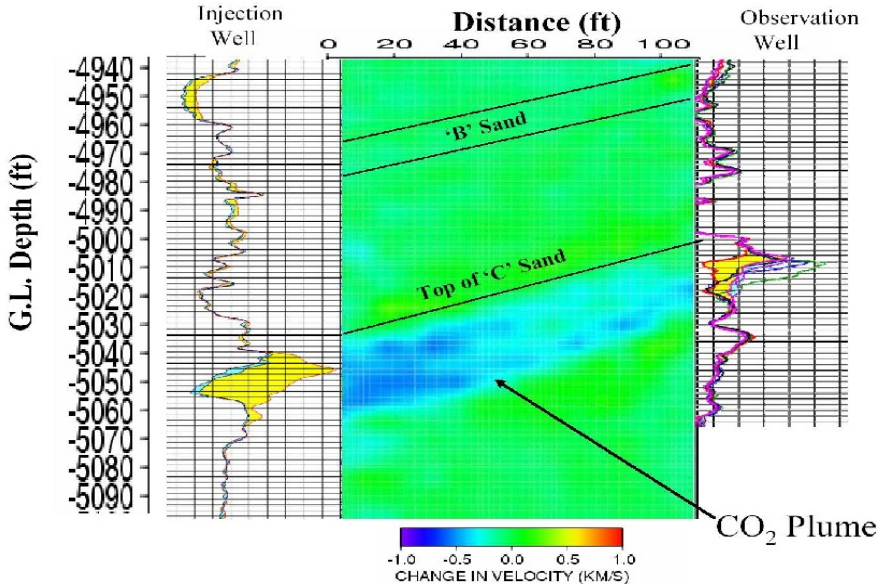


Figure 5: Tomographic image of seismic velocity change due to CO_2 injection (center) along with RST well logs for the injection (left) and monitoring (right) wells.

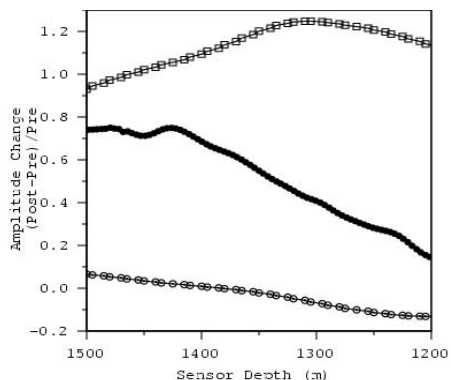


Figure 6: Comparison of measured VSP amplitude change (center) with numerical VSP model for homogeneous velocity decrease of 400 m/s (top) and variable decrease derived from crosswell for interwell region only (bottom).